NASA TECHNICAL MEMORANDUM

NASA TM X-71430

NASA TM X-71430

HOLOGRAPHIC STUDIES OF SHOCK WAVES WITHIN TRANSONIC FAN ROTORS

by W. A. Benser, E. E. Bailey and T. F. Gelder
Lewis Research Center
Cleveland, Ohio

TECHNICAL PAPER proposed for presentation at Nineteenth International Gas Turbine Conference sponsored by the American Society of Mechanical Engineers Zurich, Switzerland, March 30 - April 4, 1974

HOLOGRAPHIC STUDIES OF SHOCK WAVES WITHIN TRANSONIC FAN ROTORS

by W. A. Benser, E. E. Bailey and T. F. Gelder

National Aeronautics and Space Administration
Lewis Research Center
Cleveland, Ohio

E-7622

ABSTRACT

NASA has funded two separate contracts to apply pulsed laser holographic interferometry to the detection of shock patterns in the outer span regions of high tip speed transonic rotors. The first holographic approach used ruby laser light reflected from a portion of the centerbody just ahead of the rotor. These holograms showed the bow wave patterns upstream of the rotor and the shock patterns just inside the blade row near the tip. Much of the region of interest was in the shadow of the blade leading edge and could not be visualized. The second holographic approach, on a different rotor, used light transmitted diagonally across the inlet annulus past the centerbody. This approach gave a more extensive view of the region bounded by the blade leading and trailing edges, by the part span shroud and by the blade tip. These holograms showed the passage shock emanating from the blade leading edge and a moderately strong conical shock originating at the intersection of the part span shroud leading edge and the blade suction surface. Due to a limited viewing angle, the bow waves upstream of the rotor could not be observed, and only limited details of the trailing edge shocks were obtained. The results of these studies were extremely promising. Reasonable details of the shock patterns were obtained from holograms which were made without extensive rig modifications. These studies indicated several advancements

that would give even better results. Larger viewing windows, and holographic plates would permit a wider viewing angle and give much more coverage of the regions of interest. Shorter time delay for double-pulsed holograms is also desirable. This would minimize blade movement and give clearer holograms. With these improvements of technique effective visualization of shock configurations at least outboard of part span shrouds should be possible. Accurate definition of shock configurations will aid in attainment of improved transonic fan and compressor rotors.

INTRODUCTION

Present day transonic fan and compressor rotor blade rows operate with supersonic velocities relative to the blades over a large part of the blade span. Blade blockage and velocity diffusion combined with supersonic inlet relative velocities lead to strong shock wave systems in the blade tip regions. To minimize shock losses, it is desirable to maintain a system of weak oblique shocks or compression fans as opposed to strong normal shocks. Achievement of low loss shock systems requires an effective three-dimensional design system which accounts for equilibrium of flow throughout the fan or compressor. Some progress has been made towards development of fully three-dimensional design procedures, but the most common design systems currently in use consist of iterative calculations in separate planes. First, an axisymmetric calculation is made to determine the stream surface locations in the meridional plane. Then the flow patterns in the blade-to-blade plane are defined for a number of the streamlines determined in the axisymmetric plane. For each blade-to-blade plane an assumption is made with regard to the shock pattern

for that section, and the blade shape is selected to provide that shock pattern. Solutions between the meridional and blade-to-blade planes are iterated until consistency of axial distribution of work input is achieved.

Success of this quasi three-dimensional design system is dependent on achieving the shock configurations assumed in the design of each blade section. This system, however, has a severe shortcoming in that the shock for each spanwise section is considered separately, whereas in operation the shocks from one section to another must form continuous surfaces. Furthermore, equilibrium of pressure must be maintained throughout the flow. The equilibrium of pressure considered in the meridional plane solution is based on axisymmetric flow and does not account for discontinuities of pressure across shock waves. If the assumed shock configurations are not consistent with equilibrium requirements, the desired flow and, therefore, performance will not be obtained.

To aid in the development of high performance designs, it is desirable to know the actual shock patterns and flow conditions within the rotor blade rows. Because of the high centrifugal force fields that exist in high speed fan and compressor rotors, only limited success has been achieved with actual flow measurements. In recent years, high response pressure transducers mounted over the rotor blade tips have been used to obtain pressure contours for the blade tip section.[1] Interpretation of these contours has been complicated by the wall boundary layers, tip leakage vortices, and by the blade-to-blade and revolution-to-revolution variations of flow. Correlation between static pressure rises, inlet Mach numbers, and shock angles have been very poor. Therefore, at best,

[1] Numbers in brackets designate references at the end of paper.

this approach gives qualitative data with regard to shock patterns at the very tip of the rotor blades.

Many techniques have been considered in a search for better methods of determining the three-dimensional flow patterns in high speed rotating blade rows. These include laser-doppler velocimeters, hot-wire anemometry, several reflected light schemes, and holography. NASA chose holography as a promising approach that could be applied without excessive development. Two contracts were awarded to apply holography to two separate existing high speed transonic fan rotors. The first approach used diffuse laser light reflected from a portion of the centerbody just ahead of the rotor inlet.[2] It was applied to a 548.6 meters per second (1800 ft/sec) tip speed transonic fan rotor which was designed to use precompression to reduce losses in the rotor blade tip region.[3, 4] The second approach used light transmitted diagonally across the inlet annulus past the centerbody.[5] The fan rotor for these tests was a low loading, 488.6 meters per second (1600 ft/sec) tip speed stage designed with two weak oblique shocks in the tip region.[6, 7] In the reflected light program, only short double-pulsed holograms were made. In the transmitted light program, both short and long double-pulse holograms and scattered light holograms were made. For short double-pulsed holograms, the laser is fired twice with a very short time interval between pulses. For long double-pulsed holograms, the first pulse is made at a low rotor speed to obtain a reference field and the second pulse is made at a higher rotor speed. For the scattered light holograms, the flow was seeded with small particles. The laser was fired twice within a short time interval, and local velocities were measured by observing in the hologram reconstruction

the displacement of individual particles. In both investigations high response pressure transducers were installed over the rotor blade tip to obtain pressure contour data for comparison with holographic data. Neither stage had inlet vanes.

This paper will discuss briefly the results of the holographic data obtained, and the significance of this approach as a tool to improve design of high speed transonic fan and compressor rotors. Comparisons of tip shock patterns indicated from pressure transducer data and from holograms will be made, and suggestions for obtainment of more complete data from the holographic approach will be discussed. Details of the holocameras used are given in references 2 and 5, and general details of holography are given in references 8, 9, and 10. This paper will concentrate on results obtained rather than on the principles of holography.

TRANSONIC RESEARCH ROTORS

The reflected light holographic program was conducted by Pratt and Whitney Aircraft, and used a highly loaded, high tip speed research rotor from another NASA contract. Pertinent design variables for this rotor were as follows:

Tip speed	548.6 m/sec (1800 ft/sec)
Tip diameter	0.84 m (33.1 inches)
Specific flow	188.9 kg/m^2sec (38.7 lb/ft^2sec)
Corrected flow	78.8 kg/sec (173.8 lb/sec)
Rotor inlet hub-tip ratio	0.5
Rotor pressure ratio	2.28
Number of rotor blades	38

This rotor used precompression type blade sections for the outer 63 percent of the span and multiple circular arc blading for the inner 32 percent of blade span. There was a transition region between these two types of blade shapes. The objective of the precompression type blade is to minimize losses by designing for a series of weak shocks instead of a strong normal passage shock. A schematic of the blade section is shown in figure 1. The effective blade section in this sketch is indicated by the dotted lines. The actual blade section as shown by the solid lines was obtained by subtracting a calculated boundary layer displacement thickness from the effective profile. From points A to B on the suction surface of the airfoil, the effective surface follows a calculated free streamline along which no energy is added to the fluid. Point B represents the origin of the first captured Mach wave. B to C is the precompression section of the blade and is shaped to provide a series of weak compressions which are focused just inside the leading edge of the adjacent blade. The objective of these precompressions is to reduce the strength of the passage shock and thereby reduce total losses. From C to D the effective suction surface is designed to adjust the flow direction to be compatible with the conditions for the strong oblique shock so that no reflections exist. Flow downstream of the strong oblique shock is subsonic and the effective blade section from D to F is set to provide the proper leaving flow angle. The effective pressure surface of the blade follows a free streamline from A to E, and is then smoothly faired from E to F. The rotor had a part span shroud at 65 percent span from the hub.

Tests were made for a complete stage consisting of a rotor and stator, but only rotor performance is considered in this paper. Complete

aerodynamic and mechanical design details for this stage are given in reference 3. The overall performance of this rotor is given in figure 2 taken from reference 4. Design values of pressure ratio and efficiency are shown by the solid symbols. As can be seen at design corrected speed, the flow was higher than design, and the rotor stalled at about design pressure ratio. The maximum efficiency of 84.8 percent at design speed was considered good for a test rotor with this high tip speed and high blade loading. A study of radial distribution of pressure ratio, however, shows that the tip section did not achieve design pressure ratio even at the stall point. Therefore, even though the overall performance of this stage is good, it is obvious that design flow conditions were not achieved in the high speed tip region of the blades.

Transmitted light holography was applied to a low loading, high tip speed rotor designed and tested for NASA by the AiResearch Division of the Garrett Corporation. The holography work was conducted by TRW Systems as a subcontractor to AiResearch. Details of the rotor design were as follows:

Tip speed	488.6 m/sec (1600 ft/sec)
Tip diameter	0.73 m (28.74 inches)
Specific flow	205.1 kg/m^2sec (42 lb/ft^2sec)
Corrected flow	67.09 kg/sec (147.9 lb/sec)
Rotor inlet hub-tip ratio	0.5
Rotor pressure ratio	1.512
Number of rotor blades	40

This design used weak oblique shocks in the high Mach number tip region to minimize losses. A schematic of the blade sections in the tip region is given in figure 3. Again the dotted lines represent the effective blade surface, and the solid lines the actual blade surface as obtained by application of boundary layer displacement thickness corrections. From A to B the effective surface follows a free streamline. B is the emanation point of the first captured Mach wave. From B to C, the effective suction surface follows a free streamline. C is the point of intersection of the weak oblique leading edge shock and the suction surface. The effective surface at point C bends sufficiently to cancel the weak oblique shock and prevent any reflected shocks or expansions. From C to D the effective surface follows a free streamline. A second weak oblique shock enamates from the trailing edge, point D, and is cancelled on the pressure surface at point E. The sharp corners at C and E are rounded slightly on the actual blade to improve off design operation. The pressure surface from A to E is defined by a third degree polynomial, and from E to D it is defined by a free streamline. The rotor blades had a part span shroud at 70 percent span from the hub. The design relative discharge flow was just sonic at the spanwise location of the shroud. A complete description of the aerodynamic and mechanical design is given in reference 6.

Tests were made of a complete stage consisting of a rotor and stator. For this paper only rotor performance is considered. Rotor and complete stage performance are given in reference 7. The overall performance of the low loading-high tip speed rotor is shown in figure 4. At design speed and pressure ratio, the flow was 4 percent above design, and the efficiency at this point was 85 percent. The peak efficiency at design

corrected speed was 90 percent. Design flow and pressure ratio were obtained at a corrected speed of 94 percent of the design value. At 90 percent speed, the peak efficiency has dropped to 86 percent, and at lower speeds, the peak efficiency increases to 92 percent. This dip in the peak efficiency is due to the change in shock configurations with starting of the supersonic flow in the rotor blade tip region. The rotor starting condition is shown by the holograms which will be discussed later.

TIP TRANSDUCER RESULTS

High response pressure transducers located over the rotor blade tips have frequently been used to define shock patterns at the rotor blade tip.[1] For both stages discussed herein, ten transducers were distributed axially from a point somewhat upstream of the rotor blade trailing edge to a point somewhat downstream of the rotor blade trailing edge as shown in figure 5. Conventional static pressure taps were also located at each axial station to provide an average level of wall static pressure. The high response pressure transducers are used to measure the fluctuating component of static pressure. This is added to the time averaged pressure measured by the conventional wall static pressure taps to obtain the actual fluctuating static pressures. Typical time traces of fluctuating pressure are also shown on figure 5. These pressure traces are first indexed to the circumferential blade position and then used to obtain contours of constant pressure in the blade-to-blade space.

The resulting contour plot for a near design point for the 548.6 m/sec rotor is given in figure 6. The contours on this and succeeding similar plots are given in psia rather than S. I. units to be consistent with the references and because the gradients are more significant than absolute

magnitude for this discussion. Shock waves should appear on this figure as a coalescence of contours. Interpretation of these contours is rather difficult as many contours are normal rather than parallel to the anticipated shock directions. Based on design intent, there should be a series of weak compression waves in the region bounded by the dot-dashed lines, and a strong oblique passage shock at the location indicated by the dashed line. These waves are not clearly defined by the pressure contours, but the general levels of pressures in the entrance region are somewhat consistent with a series of shock waves. The pressure contours within the passage show a reacceleration after the forward passage shock particularly on the pressure surface. This is followed by a second shock near the passage exit. This is shown by the dotted line.

Results for the 488.6 m/sec rotor at a near design pressure ratio operating point are shown in figure 7. As for the higher speed rotor, there is no well-defined pattern of shocks shown on the contour plot. The dashed lines follow the general location of the tip section shock specified in the blade design. One could surmise the existence of rather weak shocks along the dashed lines shown on the figure.

It is clear from figures 6 and 7 that tip pressure transducers do not give an undeniable picture of even the tip shock patterns. The patterns are obscurred by such factors as wall boundary layers, finite size pressure transducer active surfaces, blade-to-blade variations of patterns, tip leakage vortices, and a general difficulty of indexing data from several transducers located at different circumferential locations. A single plot does not generally give a clear picture of tip flow conditions. Comparisons of plots for various flow conditions,

however, do show trends of shock pattern changes, and tip transducers have been effective in defining passage unstart and trailing edge shocks. The tip shock patterns shown in reference 1 are much more definitive than those defined in figures 6 and 7. The data of reference 1, however, was for a somewhat lower blade passing frequency and for stronger shocks. Both these factors would lead to better definition of shock patterns.

HOLOGRAPHIC TECHNIQUES

The first holographic technique of the program reported herein utilized diffuse light reflected from the centerbody just ahead of the fan rotor inlet face. A schematic of the light path is shown in figure 8. The illuminating beam enters the test fan through a small forward window, is reflected from the stationary hub, passes outward through the blade tip section, through the viewing window, and onto the holographic plate. The remainder of the holocamera details are given in reference 2 and will not be discussed herein. Figure 9 is a conventional photographic view of the rotor and hub section taken without the rotor tip viewing window in place. From this view it can be seen that the view of the blade passage is severely limited by the shadowing effect of the blade leading edges. Holographic techniques will increase the viewing angle over that seen in figure 9, but even so, only the entrance region of the passage can be studied with this light path arrangement. These limitations were recognized at the outset of the program, but the simplicity of installation of reflected light holography made it an attractive approach to study.

To make a hologram with this setup, the fan operating point was set. Then the laser was pulsed twice at a time interval of about 10 microseconds. In this time interval the blade passage density field moves about 10

percent of a blade passage, and the resultant double exposure gives a differential interferogram which defines density variations. The double pulsed approach cancels out the effect of imperfections in the windows. Therefore, low quality plastic windows can be used as long as there is no movement of the windows between laser pulses.

The second holographic technique was originally designed to transmit the scene beam into the hub through a strut, reflect this beam axially to the fan inlet face, and then reflect it outward through a window in the centerbody, and through the blade tip region onto the holographic plate. This scheme was abandoned because it was difficult to mount the optics within the centerbody and still maintain a low level of optics vibrations, and because this system had the same limits of viewing angle as the reflected light system. Therefore, a system was evolved which transmitted diffuse light diagonally across the inlet as shown schematically in figure 10. In this technique light enters the test fan through the large window ahead of the rotor inlet, passes by the centerbody, through the blade tip region, and out through the window over the blade tip onto the hologram plate. Details of this holographic system and its installation are given in reference 5. In this program three types of holographic procedures were tried. The most successful was a rapid double pulsed approach in which the fan operating condition was set and the laser pulsed twice at a time interval on the order of 5 microseconds. In the second approach, called the long double-pulsed approach, an operating condition was set at about 60 percent speed and the first exposure was made. The fan was then accelerated and set at a second speed condition (near design speed) and a second exposure made. Window movement led to extraneous

fringe patterns and made interpretation of this type hologram ineffective. As a result, only a limited amount of effort was applied to this approach. This approach will not be covered further in this paper. Further details, however, are given in reference 5.

The third approach was to seed the flow with 30 micron diameter glass microballoons and then double pulse the laser at a short time interval. Scattered laser light reflected from the microballoons was recorded and stream velocity could be calculated from displacement of a specific microballoon and a knowledge of the time between pulses. If a sufficiently wide viewing angle is obtainable, the axial, radial and tangential components of velocity can be approximated by this technique. Because the pulse duration of the laser was on the order of 50 nanoseconds, clear definition of the microballoon could only be obtained at very low velocities. With a rotor speed of 8 percent of design and a time delay between laser pulses of 40 microseconds, displacement at individual microballoons could be determined. Holograms made at this low speed indicated promise for this technique. Application of this scattered light approach to higher speeds will require much shorter laser pulse times. These can be achieved by using pulse choppers. However, the addition of such equipment was beyond the scope of the reference program.

REFLECTED LIGHT HOLOGRAPHIC RESULTS

A series of holograms covering a range of corrected speeds and operating pressure ratios were made on the high speed, high loading research stage. These holograms were made using the short double pulsed technique. With a sufficiently wide viewing angle, these holograms should produce a complete interference fringe pattern from which density variations within

the rotating blade passage could be determined. Due to limitations in viewing angle imposed by the rig geometry, only abrupt changes in density such as occur across shock waves can be determined. In the pictures obtained from the holograms, changes in fringe spacing occur where large density changes such as the density increase across a shock wave exist. The holograms obtained in this study were analyzed to obtain a three-dimensional location of shock systems in the rotor blade tip region.

To determine shock locations, the holograms were set up in a laser system, and photographs were taken from five different viewing angles with the lens system focused at each of several different radial positions in the blade passage. Figure 11 is a typical photograph of this type. This photograph was taken from a hologram made at a maximum flow condition at design corrected rotor speed. The camera was focused on a plane about 38 millimeters in from the blade tip. The rectangular grid is from the reference lines on the outer window. These lines are fuzzy because they are out of focus. Bow waves from two blades are clearly visible as variations in fringe spacing. An oblique passage shock is also indicated by a change in fringe spacing. Bow waves could be detected to a point forty percent of span from the hub. The leading edge of the rotor blade restricted the view of the passage shock to the outer 20 percent of the passage depth. By viewing a specific shock wave at various radial positions and from various angles, the plane of the shock wave was determined. Sketches of shock locations for several different radial positions for a maximum flow point at design speed are shown in figure 12.

From these sketches it is obvious that the passage flow is started in the tip region because the bow waves emanate from points close to the

leading edge, and the passage shocks near the tip are swept back into the passage.

Schematics of the shock patterns for a 70 percent speed, intermediate flow point are shown in figure 13. For this speed and flow a bow wave appears attached at 100 percent span (tip section) which is not apparent at 69 percent span. The effect of the precompression ramp is evident by a strong, almost normal shock standing appreciably ahead of the blade leading edge and across the passage. Further data from these tests are given in reference 2.

The reflected light system of holography does give a good picture of bow waves, but the limited field of view available severely limits the portion of the blade passage that can be studied. Larger windows and larger holograms plus variations of circumferential blade positions for taking holograms would help increase the viewing area, but the shadowing by the blade leading edge would still impose a rather severe limitation to the extent of blade passage that can be studied.

TRANSMITTED LIGHT HOLOGRAPHIC RESULTS

With the transmitted light holography using the short double pulsed technique, holograms were taken of the 488.6 m/sec rotors for a range of speeds and flows. For some of the operating points, holograms were taken with the rotor blades in different positions with respect to the viewing window. Several techniques to analyze the resultant holograms were tried. These included mounting the hologram in a laser light system and photographing the image through the hologram, mounting a photographic plate in the image field, and simply viewing the image field by eye. The latter scheme proved most effective when an actual set of blades was mounted in

the image field and the magnification of the image was set to match the blade scale. A photograph of the blades in the image field is shown in figure 14. By placing wires on the observed shock planes in the model blades in the image plane, the locations of specific shock planes can be defined. Viewing from several angles and using holograms with the blades in various positions with respect to the viewing window aids materially in defining the shock plane locations. After the shock planes were completely defined by the system of wires, a model was made using sheets of transparent plastic to define the various shock planes.

Figure 15 shows two views of the blade model with shock waves for a 100 percent corrected speed operating point and a pressure ratio near design. The holographic viewing angle for these tests was too small to permit observations of the bow waves forward of the blade leading edge. Therefore, only shocks within the actual blade passage are shown. This model also shows a tip leakage vortex along the suction surface at the tip. This tip leakage vortex tends to obscure shock definition near the suction surface in the tip region. There is a rather weak oblique shock starting from the blade leading edge and terminating on the suction surface near the blade trailing edge. This shock is similar to the forward passage shock specified in the design, but appears to be nearly normal to the blade at the suction surface. The design assumed that this shock was always oblique. This deviation from design intent may be due to blade boundary layer effects or to effects of the tip leakage vortex.

Another shock wave identified in figure 15 as first shroud shock, starts at the leading edge of the part span shroud and extends from blade to blade. It is swept back in the flow direction and intersects

the outer wall near the blade trailing edge. The exact leading edge of this shock at various positions across the passage cannot be determined due to a limited viewing angle, but this appears to be a somewhat conical-shaped shock emanating from the shroud leading edge on the blade suction surface. On the pressure surface and at other positions across the blade passage, this shock is ahead of the shroud leading edge. Further back in the passage a second shock is observed which appears to emanate in the region of the intersection of the part span shroud and the pressure surface of the blade. This shock very nearly coincides with the passage shock near the blade trailing edge. These part span shroud shocks obviously affect the flow in the passage in the tip region, but were not considered in the design of the blades.

From other holograms presented in reference 5, a blade trailing edge shock is also observed. This shock appears to sweep forward at smaller radii, and becomes nearly normal as the stage is throttled toward stall. Because of the limited viewing angle, definition of this trailing edge shock is not as positive as those in the forward part of the passage.

Figure 16 is a photograph of a hologram for a 90 percent speed mid-flow range point. From this view, it can be seen that at this speed the passage is not started in the tip region and the forward passage shock is a strong normal shock. This strong normal shock probably accounts for the dip in peak efficiency which is shown on figure 4 for 90 percent speed.

There was an amazing consistency of shock patterns for different holograms for a given operating condition. This was not expected because hot wire studies of blade wakes and high response tip pressure transducer data indicate large variations from blade to blade and from revolution to

revolution for the same blade. The shock patterns from holograms taken on two completely separate runs, however, showed good agreement.

More details on the results of this program are given in reference 5. In general excellent results were obtained from the short double pulsed holograms insofar as shock locations for the forward part of the passage are concerned. Details ahead of the blade row and in the trailing edge region were not so well defined. Several things could be done to improve the quality and viewing area for this type hologram. Most important would be to increase window and hologram plate size. This work was done with a three by five inch viewing window and four by five inch holographic plates. Use of much larger windows and larger holographic plates would increase the field of view and permit better evaluation of conditions in the leading and trailing edge regions of the blades. Shorter pulse separation times would reduce blade movement and provide clearer holograms.

SCATTERED LIGHT HOLOGRAMS

A limited number of holograms were made using a scattered light technique in which the flow was seeded with 30 micron glass microballoons and the laser double pulsed at a short time interval. By focusing in the hologram reconstruction on a given microballoon, measuring its movement, and knowing the time interval of exposures, a flow velocity can be obtained. Figure 17 is a photograph of a hologram taken with the camera focused at 20 centimeters in from the tip. This hologram was made at 8 percent speed. In this figure each pair of dots represents one microballoon and the distance between dots as indicated by the Δ is a measure of flow velocity at that point. The hologram from which figure 17 was made was taken at a very low rotor speed. Therefore, no shocks existed for this test condition.

At higher speeds the pulse duration was too long to obtain clear micro-balloon definition. Shorter pulse duration could be obtained, but this would require system changes which were beyond the scope of this specific program. The data obtained, however, do indicate that at least qualitative velocity measurements can be made by this technique.

COMPARISON OF TIP SHOCKS LOCATION FROM HOLOGRAMS AND TIP PRESSURE TRANSDUCERS

Rotor tip shock patterns as measured by high response pressure transducers were given for the two test configurations in figures 6 and 7. These data are for design speed operation. As noted previously, the location of passage shocks in these contour plots are not extremely exact. Figure 18 is a repeat of figure 6 for the 548 m/sec rotor with the shock locations as determined from a hologram for a comparable operating condition superimposed. The pressure transducers did not cover a sufficient distance upstream of the rotor blade leading edge to determine bow shock configurations, and the holograms did not cover much of the blade passage region. Therefore, the region of overlap for the two systems was extremely limited. A general agreement between shock locations from the holograms and regions of maximum pressure rise from the pressure contours is noted.

Figure 19 is a repeat of figure 7 for the 488.6 m/sec fan rotor with shock waves determined from the hologram at a similar operating condition superimposed. Also shown on this figure is the region of tip leakage vortex observed in the holograms. This tip vorticity may have an effect on the static pressure contours and thus complicate the interpretation of pressure contours. The region of overlap for data with this rotor is much larger than for the reflected light holograms for the higher speed rotor. The forward passage shock appears to bend in the vicinity of the

tip vortex and become almost normal at the suction surface. The shock from the part span shroud and the trailing edge passage shock intersect the outer wall in almost the same location. These two shock intersections with the outer wall are both almost normal to the mean flow path. Although the static pressure contours as obtained from the tip pressure transducer traces do not explicitly define the shock locations, the regions of maximum static pressures are in general agreement with the shock patterns defined by the holograms.

1. Miller, G. R. and Bailey, E. E., "Static Pressure Contours in the Blade Passage at the Tip of Several High Mach Number Rotors," NASA TM X-2170, Feb., 1970.

2. Hantman, R. G., et al., "Application of Holography to the Determination of Flow Conditions Within the Rotating Blade Row of a Compressor - Final Report," NASA CR-121112, PWA-4712, July 1973.

3. Morris, A. L.; Halle, J. E. and Kennedy, E., "High Loading 1800 Ft/Sec Tip Speed Transonic Compressor Fan Stage. I-Aerodynamic and Mechanical Design," NASA CR-120907, PWA-4534, 1972.

4. Morris, A. L. and Sulam, D. H., "High Loading, 1800 Ft/Sec Tip Speed Transonic Compressor Fan Stage. II-Final Report," NASA CR-120991, PWA-4463, Dec. 1972.

5. Wuerker, R. F.; Kobayashi, R. J. and Heflinger, L. O., "Application of Holography to Flow Visualization Within Rotating Compressor Blade Row," NASA CR-121264, AiResearch 73-9489, 1973.

6. Wright, L. C., et al., "High Tip Speed, Low-Loading Transonic Fan Stage - Part I Aerodynamic and Mechanical Design," NASA CR-121095, AiResearch 72-8421, April 1973.

7. Ware, T. C.; Kobayashi, R. J. and Jackson, R. J., "High-Tip-Speed, Low Loading Transonic Fan Stage. Part II Final Report," NASA CR-121263, AiResearch 73-9488, 1973.

8. Heflinger, L. O.; Wuerker, R. F. and Brooks, R. E., "Holographic Interferometry," Journal of Applied Physics, vol. 37, 1966, p. 642.

9. Siebert, L. D. and Geister, D. E., "Pulsed Holographic Interferometry Versus Schlieren Photography," AIAA Journal, vol. 6, 1968, p. 2194.

REFERENCES (Continued)

10. Witte, A. B. and Wuerker, R. F., "Laser Holographic Interferometry Studies of High Speed Flow Fields," AIAA Fourth Aerodynamic Testing Conference, Paper no. 69-347, 1969.

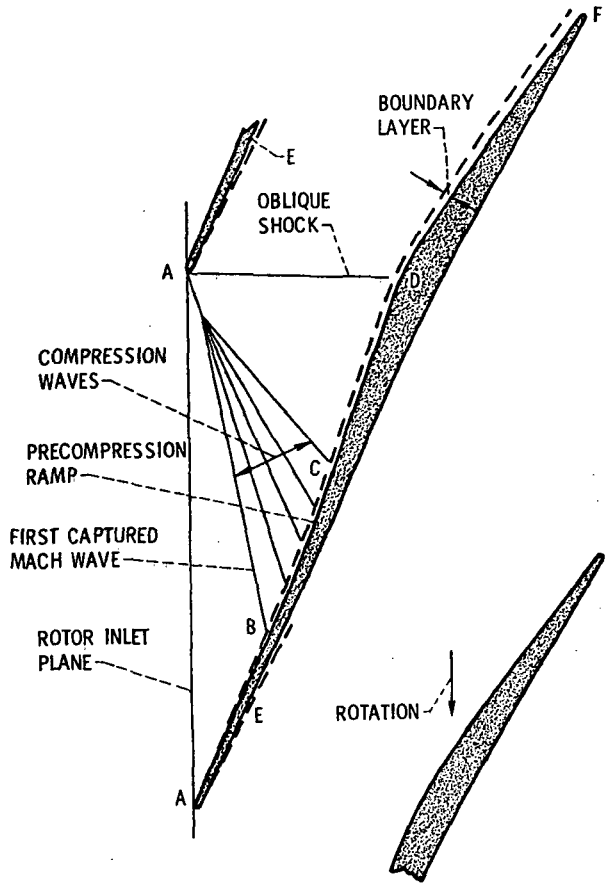

Figure 1. - Precompression blade section (548.6 m/sec rotor).

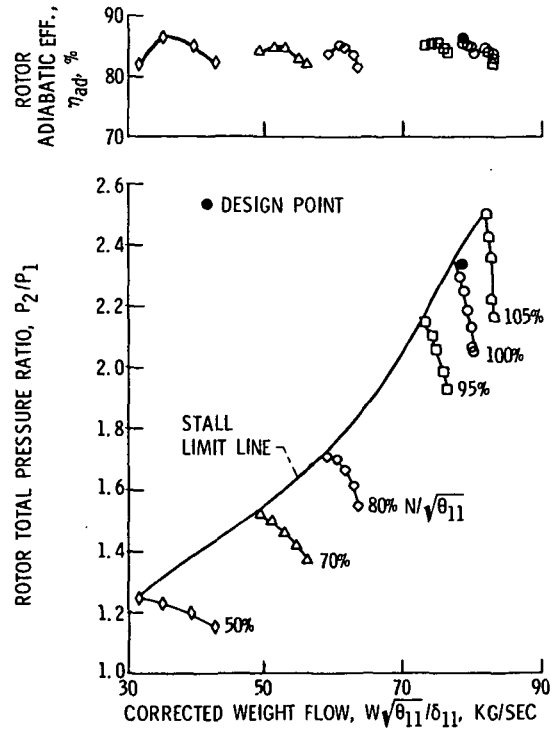

Figure 2. - 548.6 m/sec rotor overall performance with uniform inlet flow.

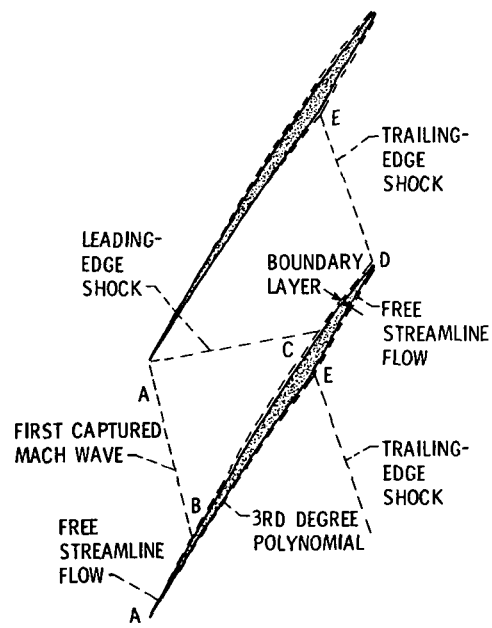

Figure 3. - Representative rotor blade section (488.6 m/sec rotor).

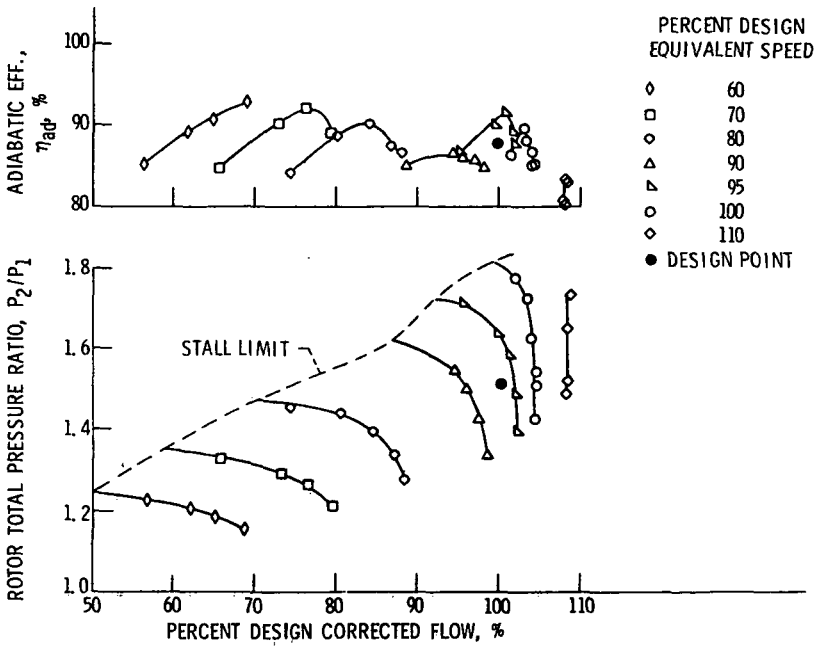

Figure 4. - 488.6 m/sec rotor overall performance with uniform inlet flow.

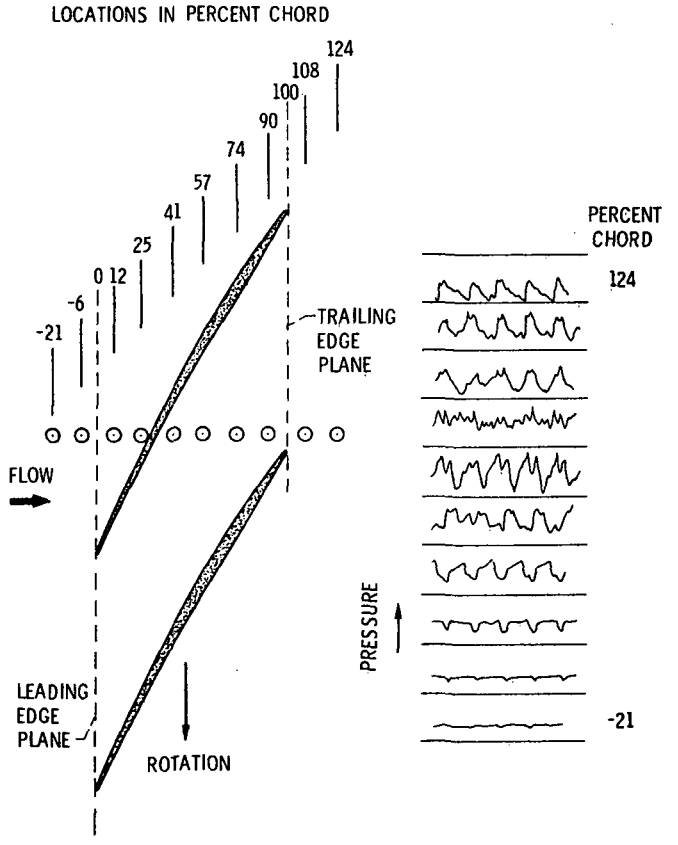

Figure 5. - Relative location of pressure transducers and typical high response casing transducer oscillograph traces.

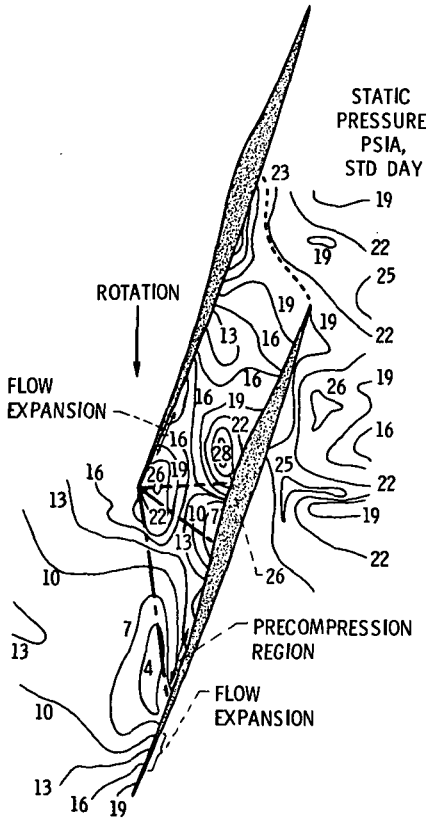

Figure 6. - 548.6 m/sec rotor blade tip static pressure contours, 100% design speed, near design flow.

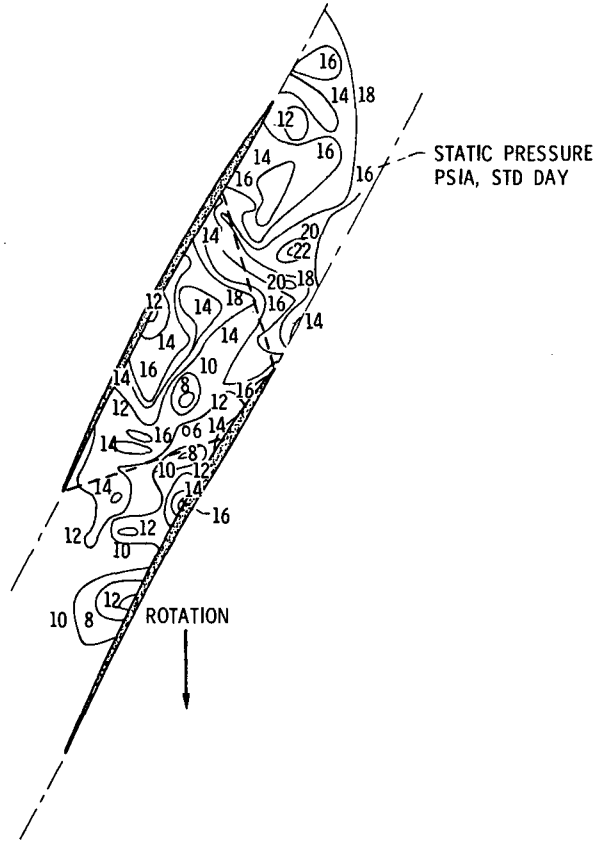

Figure 7. - 488.6 m/sec rotor blade tip static pressure contours, 100% design speed, near design pressure ratio.

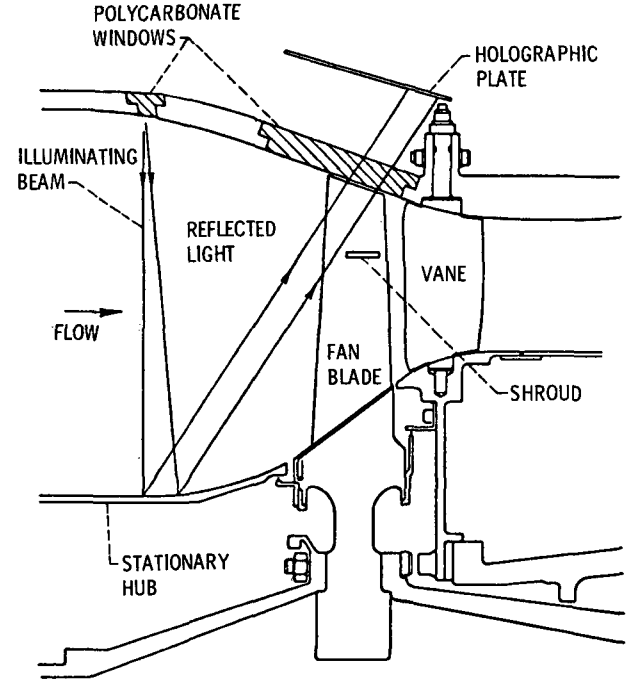

Figure 8. - Optical paths for reflected light holography.

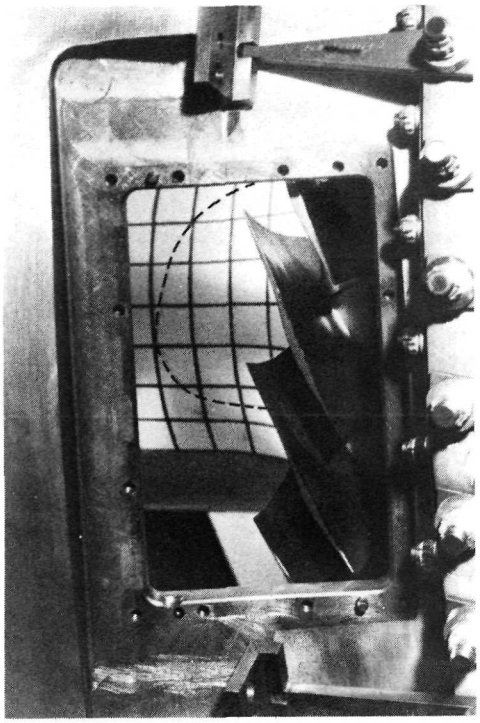

Figure 9. - Interior of reflected light holography rig as seen without window in place.

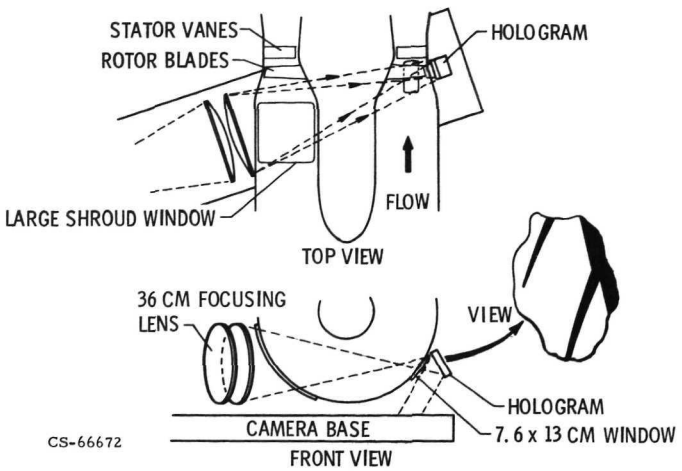

Figure 10. - Optical paths for transmitted light holography.

Figure 11. - Reflected light Hologram taked at the 100 percent speed line, maximum flow (camera focused 38 mm below tip, f 11).

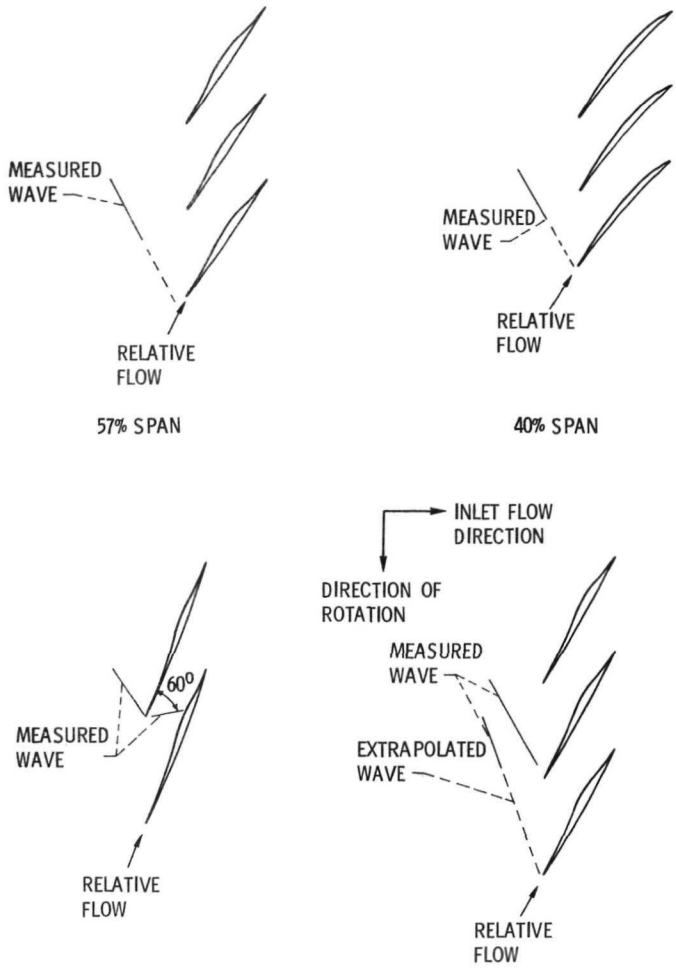

Figure 12. - Rotor shock patterns from reflected light holograms 100%design speed, maximum flow.

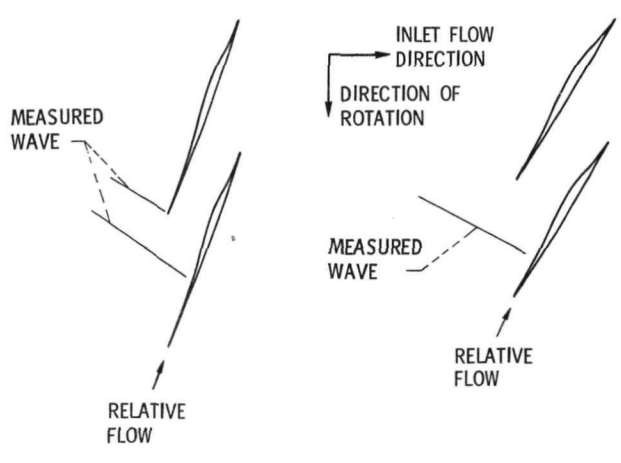

Figure 13. - Rotor shock patterns from reflected light holograms, 70% design speed, intermediate flow.

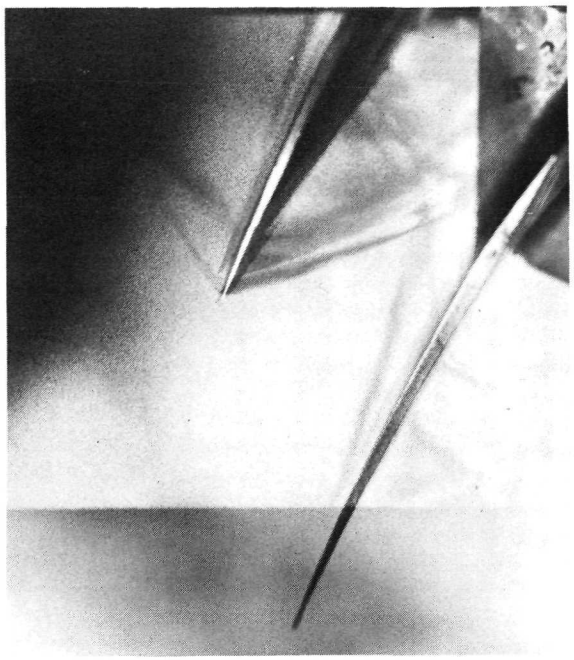

Figure 14. - View of transmitted light hologram image coincident with rotor blades.

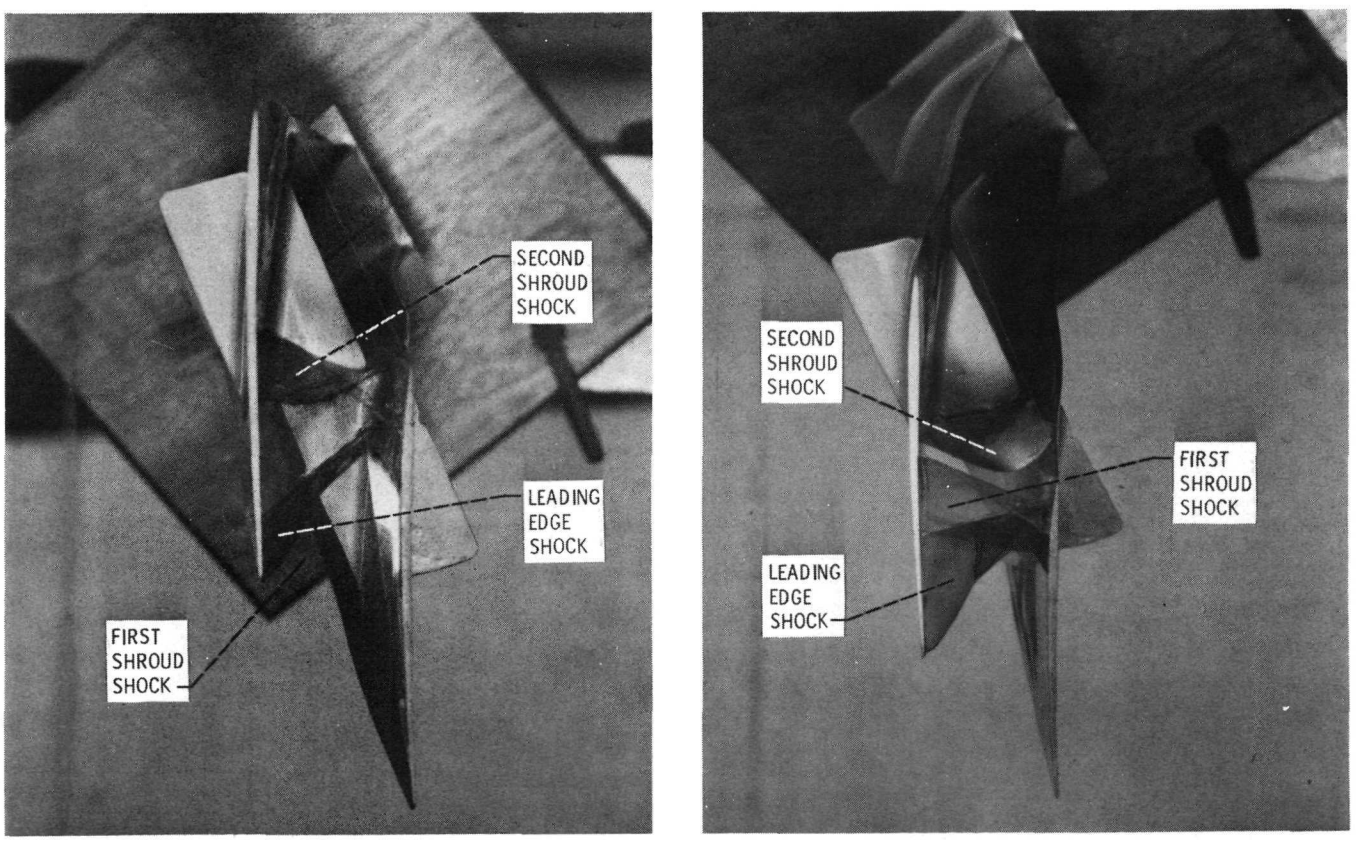

(a) TOP VIEW.

(b) REAR VIEW.

Figure 15. - Views of 488.6 m/sec rotor blade model with shock system at design speed and near design pressure ratio.

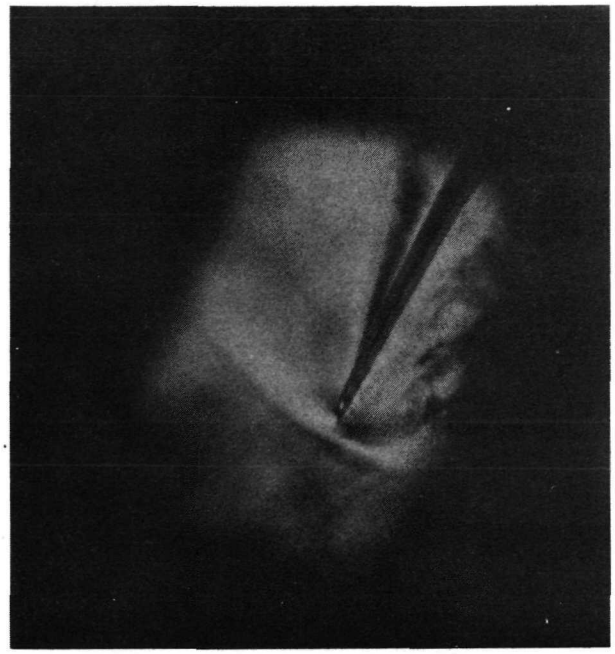

Figure 16. - View of transmitted light hologram for 90 percent speed.

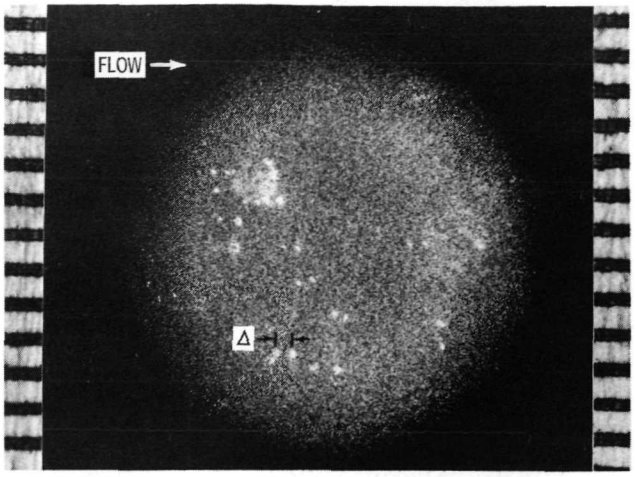

SCALE IS 1 MILLIMETER PER DIVISION (AT BORDER)

Figure 17. - Enlarged portion of reconstruction of hologram made with scattered light. (Reduced 50 percent in printing.)

E-7622

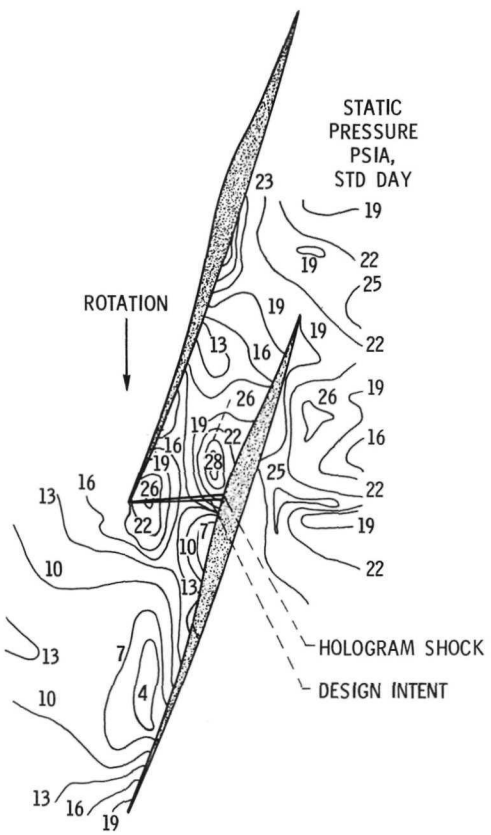

Figure 18. - 548.6 m/sec rotor blade tip static pressure contours with shocks indicated from reflected light holography.

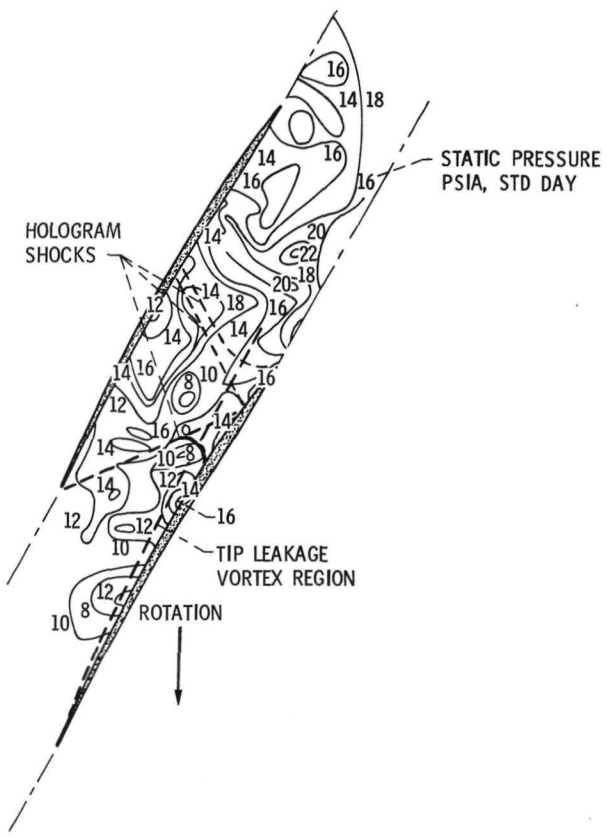

Figure 19. 488.6 m/sec rotor blade tip static pressure contours, with shocks indicated from transmitted light holography.